Chapter 15
Solid State Lasers

We discuss solid state lasers that make use of electronic states of impurity ions in a dielectric crystals or in glasses—other types of solid state lasers, namely semiconductor lasers that are based on electrons in energy bands of semiconductors, will be treated in later chapters.

We describe the principle of the ruby laser. We treat the titanium–sapphire laser in more detail than in an earlier chapter. We mention other broadband solid state lasers. Then we present a description of the neodymium-doped YAG laser, of other neodymium lasers, and of other YAG lasers. We describe disk lasers and fiber lasers. We give a short survey of solid state lasers with respect to host materials and impurities. Finally, we describe line broadening processes occurring in solid state laser media.

The active medium of a disk laser has the form of a disk rather than the form of a rod. A disk laser pumped with a semiconductor laser has a high beam quality.

Glass lasers are used for generation of near infrared radiation of different wavelengths. The neodymium-doped glass laser can produce intense radiation pulses at a wavelength at 1.05 μm. Doped glass fiber lasers generate radiation in the wavelength range 0.7–3 μm. Fiber lasers are robust and flexible. They are suitable for applications in many areas (material processing, biophysics, medicine); fiber lasers are able to generate continuous wave radiation or picosecond pulses.

15.1 Ruby Laser

A ruby laser (Fig. 15.1) uses Cr^{3+} ions in an Al_2O_3 (sapphire) crystal with a doping concentration of typically 0.05% by weight Cr_2O_3; the density of Cr^{3+} ions is $N_0 = 1.6 \times 10^{25}\ m^{-3}$. An excited Cr^{3+} ion in Al_2O_3 has two long-lived energy levels with a small energy separation. The lifetime of the levels with respect to spontaneous emission of radiation is about 3 ms. Two broad energy bands are suited as pump bands. The optical transitions between the long-lived levels and the ground state level occur at two slightly different wavelengths (R_1 fluorescence line at 694.3 nm

K.F. Renk, *Basics of Laser Physics*, Graduate Texts in Physics,
DOI 10.1007/978-3-319-50651-7_15

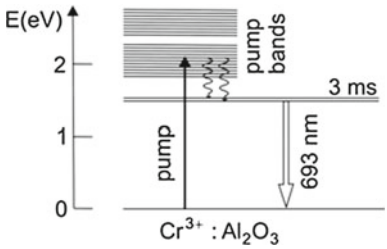

Fig. 15.1 Ruby laser (*principle*)

and R_2 line at 692.8 nm). The level splitting is due to a week trigonal crystalline field that is present, in addition to a cubic crystalline field, at the sites of the Cr^{3+} impurity ions in sapphire). The ground state level is identical with the lower laser level. By optical pumping into a pump band and fast nonradiative relaxation, the upper laser levels are populated. At sufficiently strong pumping, the populations of the upper laser levels are larger than the population of the ground state level. The gain cross section (at the center frequencies of the two lines) has the value $\sigma_{21} = 2.5 \times 10^{-24}\ \mathrm{m}^2$.

The further development of the ruby laser, after its first operation (in 1960 [120]), stimulated the development of special high-power discharge lamps (continuously working lamps and pulsed flash lamps too). Today, pumping of a ruby laser is possible with radiation of another laser. The long lifetime of the upper laser level makes it possible to excite almost all Cr^{3+} ions in a ruby crystal and to produce, by Q-switching, pulses of very large pulse energy.

15.2 More About the Titanium–Sapphire Laser

In an earlier chapter we have already introduced the titanium-sapphire laser (Ti:Al_2O_3 laser). Here, we discuss the laser in more detail.

We can describe the energy level diagram of Ti^{3+} in Al_2O_3 (Fig. 15.2, left) in a formal way. We introduce the *configuration coordinate* Q. It describes an average distance between a Ti^{3+} ion and neighboring ions. The energy of a level depends on Q. The energy curve $E(Q)$ indicates that the ground state is accompanied by vibronic levels. The energy of a vibronic level is composed of electronic and vibrational energy. Q_0 is the configuration coordinate at which the energy minimum of the electronic ground state occurs. Correspondingly, the $E^*(Q)$ curve indicates that the excited state of Ti^{3+} is accompanied by vibronic energy levels too. The configuration coordinate Q_0^* at which the energy minimum of excited Ti^{3+} occurs is larger than Q_0.

Figure 15.2 (right) illustrates the four-level description of the titanium-sapphire laser:

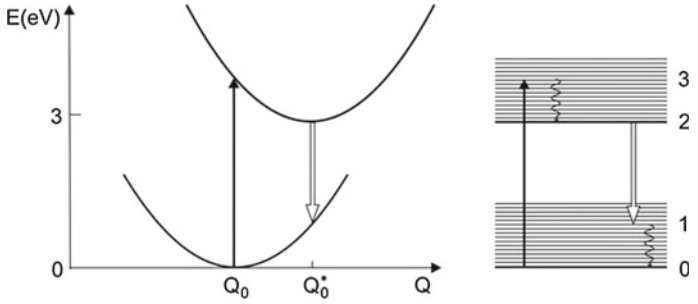

Fig. 15.2 Titanium–sapphire laser (*principle*)

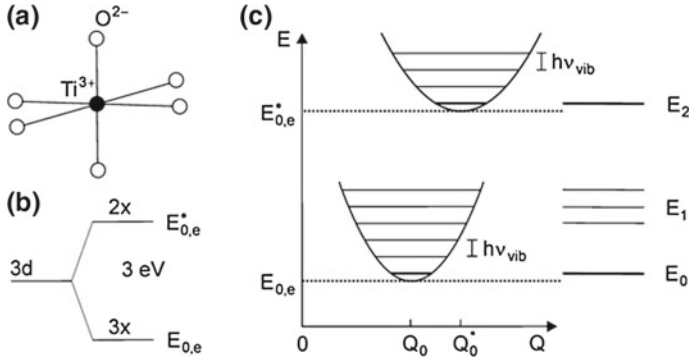

Fig. 15.3 Ti^{3+} in Al_2O_3. **a** Surrounding of a Ti^{3+} ion. **b** Crystal field splitting of the 3d state of Ti^{3+}. **c** Vibronic energy levels due to coupling to a phonon

- In an optical absorption process, a Ti^{3+} ion is excited from the ground-state level (level 0) to a vibronic level (level 3) of the electronically excited state.
- Fast nonradiative relaxation (relaxation time $\sim 10^{-13}$ s) leads to population of the lowest excited-state level (level 2) of Ti^{3+}.
- An optical transition occurs to a vibronic level of the electronic ground state.
- After fast relaxation (relaxation time $\sim 10^{-13}$ s), the Ti^{3+} ion is in its ground state.

Optical transitions are governed by the Franck–Condon principle: optical transitions occur without a change of the atomic distances.

We now discuss the origin of the vibronic energy levels of Ti^{3+} in Al_2O_3. The Ti^{3+} ion has the electron configuration $1s^2 2s^2 2p^6 3s^2 3p^6 3d$. It has filled shells (like an argon atom) and an external electron in the 3d shell. The 3d state of the free Ti^{3+} ion is fivefold degenerate according to the quantum number ($l = 2$) of the orbital momentum.

A Ti^{3+} ion in an Al_2O_3 crystal (Fig. 15.3a) is surrounded by an octahedron of oxygen ions (O^{2-} ions). In the field of the ions (crystal field), the 3d state splits

(Fig. 15.3b) into two states, one shows a threefold and the other a twofold degeneracy with respect to the electron orbital. The threefold degenerate state is the ground state of Ti^{3+} in Al_2O_3 and the twofold state is the lowest excited state; the energy level splitting is about 3 eV. These two electronic states are the basis of the titanium–sapphire laser.

An oscillation of the oxygen octahedron is associated with an oscillating electric field at the site of a Ti^{3+} ion. The field influences the orbital of the 3d electron and therefore the electron states. An oscillation of the octahedron couples to lattice vibrations of the whole crystal. Vice versa, all lattice vibrations of the Al_2O_3 crystal couple to an oxygen octahedron and therefore to the electronic states of a Ti^{3+} ion. The coupling gives rise to a distribution of electronic ground state levels as well as of excited state levels. The energy of the electronic ground state of Ti^{3+} is (Fig. 15.3c)

$$E = E_{0,e} + E_{vib}. \tag{15.1}$$

$E_{0,e}$ is the electronic energy of Ti^{3+} without oscillation and E_{vib} the energy levels. The levels are vibronic (=vibro-electronic) energy levels. The corresponding states are vibronic states.

The energy of the electronically excited state of Ti^{3+} is

$$E^* = E^*_{0,e} + E_{vib}. \tag{15.2}$$

$E^*_{0,e}$ is the electronic energy of the excited state and E_{vib} again the vibrational energy. E^* is the energy of a vibronic state of excited Ti^{3+}.

A single vibration of an Al_2O_3 crystal has the vibrational energy

$$E_{vib} = \left(v + \frac{1}{2}\right) h\nu_{vib}, \tag{15.3}$$

where ν_{vib} is a vibrational frequency, v the vibrational quantum number of this vibration, and $\frac{1}{2}h\nu_{vib}$ the zero point energy of the vibration.

An Al_2O_3 crystal has a large number of vibrational frequencies; the number of different lattice vibrations is of the order of 10^{22} for a crystal volume of 1 cm^3. Therefore, the vibronic levels have a continuous energy distribution. The different energy levels of Ti^{3+} in Al_2O_3 are:

- $E_0 = E_{0,e}$+ zero point energy of all vibrations = energy of the ground state level.
- $E_2 = E^*_{0,e}$+ zero point energy of all vibrations = lowest energy of the excited state.
- $E_1 = E_0 + E_{vib}$ = lower laser levels, having a broad energy distribution.

The spontaneous lifetime of a vibronic level of an excited Ti^{3+} ion is ~3.8 μs.

Our discussion shows that the occurrence of a broad distribution of pump levels and of a broad distribution of lower laser levels in titanium–sapphire is a consequence of the vibronic character of the energy levels of Ti^{3+} in Al_2O_3. We will derive the

gain profile of Ti^{3+}:Al_2O_3 in Sect. 17.2. Vibronic energy levels are the basis of many other lasers.

15.3 Other Broadband Solid State Lasers

We compare the titanium–sapphire laser with other broadband tunable solid state lasers (Table 15.1): alexandrite laser; Cr:LiSAF laser (chromium-doped lithium strontium aluminum fluoride laser); and Cr:LiCaF laser (chromium-doped lithium calcium fluoride laser). The wavelength λ given in the table is the wavelength of maximum gain coefficient. Titanium–sapphire has the largest gain bandwidth $\Delta\nu_g$.

The alexandrite laser was the first solid state laser that was tunable over a wide wavelength range (700–820 nm). In alexandrite ($BeAl_2O_4$ crystal doped with Cr^{3+}), the Cr^{3+} ions (concentration 3×10^{25} m^{-3}) replace about 0.1% of the Al^{3+} ions. The energy levels of Cr^{3+} in alexandrite, used in the laser, are (Fig. 15.4) the following:

- 0; ground state. Q_0 is the configuration coordinate of the energy minimum of the vibronic ground state levels.
- 1A; vibronic band of the ground state.
- 2A; vibronic band of excited Cr^{3+}; spontaneous lifetime 1.5 ms.
- 2B; another vibronic band of excited Cr^{3+}, 70 meV above the 2 A band; spontaneous lifetime of 1.5 µs. $Q_0^\star$ is the configuration coordinate of the energy minimum of this vibronic band.

Table 15.1 Tunable lasers

Lasers	λ (nm)	τ_{sp} (µs)	σ_{21} (m^2)	$\Delta\nu_g$ (THz)	Tuning range (nm)
TiS	790	3.8	3×10^{-23}	110	660–1,180
alexandrite	760	260	10^{-24}	50	700–820
Cr:LiSAF	850	70	5×10^{-24}	80	780–1,010
Cr:LiCaF	780	170	13×10^{-24}	60	720–840

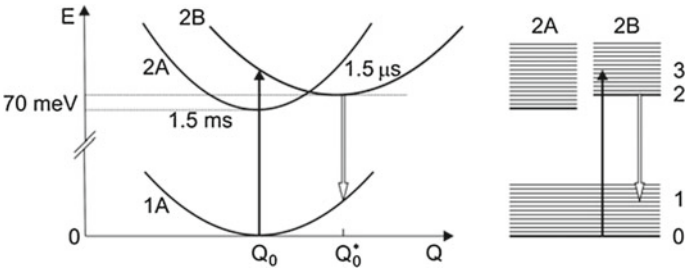

Fig. 15.4 Alexandrite laser

- 2; upper laser level (belonging to 2B); spontaneous lifetime 1.5 μs.
- 1; lower laser level (vibronic level belonging to 1A).
- 3; pump levels (belonging to 2B), pumped with radiation around 680 nm.

Optical pumping and fast relaxation result in populations of the 2A and the 2B vibronic bands. The population of each of the vibronic bands is in thermal equilibrium and the populations of the two bands are in thermal equilibrium with each other. The equilibrium is determined by the crystal temperature. To obtain a large population of 2B levels, the crystal is kept at an elevated temperature (60 °C or higher). Laser transitions occur around a wavelength of 760 nm within a width of about 100 nm.

The energy levels of Cr^{3+} in LiSAF and LiCaF are similar to the energy levels of Cr^{3+} in alexandrite. There is, however, an important difference: the energy minimum of the 2B band lies below the minimum of the 2 A band. Therefore, heating of the crystals is not necessary.

Alexandrite, Cr^{3+}:LiSAF, and Cr^{3+}:LiCaF lasers can be used for the same tasks as the titanium–sapphire laser. Titanium–sapphire has the advantage that the crystalline material has a larger hardness and a higher heat conductivity.

15.4 YAG Lasers

A Nd:YAG laser (YAG = $Y_3Al_5O_{12}$ = yttrium aluminum garnet) can have a high beam quality and can be operated as a cw or as a pulsed laser. Applications:

- Material processing: drilling, point welding, marking.
- Medicine: surgery, (Nd:YAG laser radiation can be guided with a glass fiber into the interior of a body and focused by a lens); eye surgery; applications in dermatology, *see*, for instance [127–129].

A neodymium YAG laser (Fig. 15.5a) makes use of energy levels of Nd^{3+}. The Nd atom has the electron configuration $4f^35s^25p^66s^2$. The free Nd^{3+} ion has the configuration $4f^25s^25p^6$; the two lowest energy levels are $^4I_{9/2}$ and $^4I_{11/2}$. The crystalline

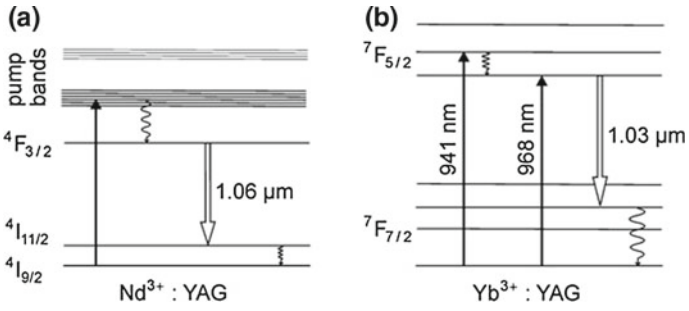

Fig. 15.5 YAG lasers. **a** Neodymium-doped YAG laser. **b** Ytterbium-doped YAG laser

Table 15.2 YAG lasers

Laser	λ	λ_{pump} (nm)	τ_{sp} (μs)	$\Delta\nu_g$	σ_{21} (m^2)
Nd:YAG	1.06 μm;	808	230	140 GHz	3×10^{-22}
Yb:YAG	1.03 μm;	941 968	960	1.7 THz	2.1×10^{-24}
Pr:YAG	1.03 μm	941			
Er:YAG	2.94 μm	800 970			

electric field causes a splitting of these levels (not shown in the figure). Energetically higher lying levels serve for optical pumping. Optical pumping and fast relaxation leads to population of the long-lived $^4F_{3/2}$ level (spontaneous lifetime 230 μs). The laser transition $^4F_{3/2} \rightarrow {}^4I_{11/2}$ corresponds to a wavelength of 1.064 μm (frequency ∼300 THz).

YAG crystals can be prepared in a very high crystal quality. Nd^{3+} ions can replace about 1% of the Y^{3+} ions. Optical pumping of a neodymium YAG laser is possible with a lamp or with a semiconductor laser. Depending on the size of a laser crystal, a neodymium YAG laser can produce laser radiation at power levels of 1–10 W or more. Operated as a giant pulse laser, a Nd:YAG laser can generate pulses of an energy of 1 J.

Other laser frequencies of the Nd^{3+}:YAG laser lie at 0.914 μm. ($^4F_{3/2} \rightarrow {}^4I_{9/2}$ transitions) and at 1.35 μm ($^4F_{3/2} \rightarrow {}^4I_{13/2}$ transitions).

Table 15.2 shows a list of various other YAG lasers.

- *Ytterbium-doped YAG laser* (Fig. 15.5b). The ytterbium-doped YAG laser (Yb:YAG laser) emits at 1.03 μm, it is pumped with radiation (at 940 nm) of a semiconductor laser (InGaAs laser) by transitions between $^7F_{3/2}$ sublevels and $^7F_{5/2}$ sublevels. The Yb^{3+} ions can replace 6% of the Y^{3+} ions in YAG. The ytterbium-doped YAG laser is becoming a competitor of the neodymium-doped YAG laser. Due to a high concentration of impurity ions, ytterbium-doped YAG crystals are especially suited as active media of lasers of small length (namely disk lasers, Sect. 15.6).
- *Praseodymium-doped YAG laser*. Pr^{3+} ions replace Y^{3+} ions. The doping can be extraordinarily high; it is possible to replace about 26% of the Y^{3+} ions by Pr^{3+} ions. The Pr:YAG laser, pumped with radiation of a semiconductor laser, emits infrared radiation.
- *Erbium-doped YAG lasers* (Fig. 15.6). The free erbium (Er) atom has the configuration $[Xe]4f^{12}5s^25p^66s^2$. Removing three electrons leads to Er^{3+} with the electronic configuration $[Xe]4f^{11}5s^25p^6$. The Er^{3+} ion, doped into a solid, has a long-lived excited state $^4I_{11/2}$. Laser transitions, $^4I_{11/2} \rightarrow {}^4I_{13/2}$, generate infrared radiation (wavelength 2.94 μm). Pumping of the erbium-doped YAG laser, via the narrow $^4I_{11/2}$ or $^4I_{9/2}$ levels, is possible with a semiconductor laser (at 980 nm or 800 nm); it is possible to operate an erbium-doped YAG laser at 1.54 μm as a three-level laser (of ruby laser type).

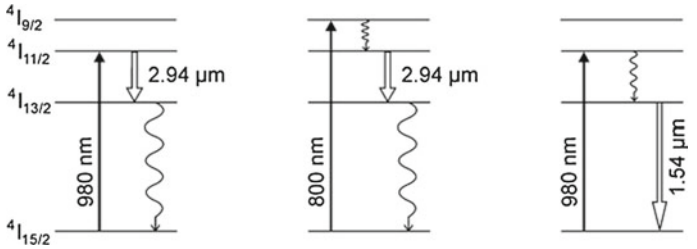

Fig. 15.6 Erbium-doped YAG lasers

The erbium-doped YAG laser with emission of radiation at 2.94 μm is of interest for biomedical applications.

15.5 Different Neodymium Lasers

Various other solids doped with Nd^{3+} are suitable as active media (Table 15.3).

- The Nd:YVO_4 laser emits at the same wavelength (1.064 μm) as the Nd^{3+}:YAG laser. With respect to applications, the Nd^{3+}:YVO_4 laser competes with the Nd^{3+}:YAG laser.
- Nd:YLF laser (= Nd:$LiYF_4$ = neodymium-doped lithium yttrium fluoride laser). The laser emits at 1.047 μm and 1.053 μm. Pumping is possible with a semiconductor laser (pump band at 804 nm, halfwidth 4 nm). The laser is also an alternative to the Nd:YAG laser.
- Neodymium-doped glass laser. In glass, Nd^{3+} ions occupy sites with different surroundings and different crystal fields. This leads to an inhomogeneous broadening of the excited-state levels. The halfwidth of the corresponding line (∼6 THz) allows for generation of picosecond pulses. There are broad pump bands around 750 and 810 nm.

The lasers can generate radiation at power levels in the 10–100 W range.

Table 15.3 Neodymium-doped solid state lasers

Laser	λ (μm)	λ_{pump} (nm)	τ_{sp} (μs)	$\Delta\nu_g$	σ_{21} (m^2)
Nd:YAG	1.064	808	230	140 GHz	2.8×10^{-22}
Nd:YVO_4	1.06	809	90	210 GHz	$1.1 \times 10^{-22}(\pi)$ $4.4 \times 10^{-23}(\sigma)$
Nd:YLF	1.047 1.053	804	480	200 GHz	1.8×10^{-23} 1.2×10^{-23}
Nd:glass	1.05		300	6 THz	3×10^{-24}

15.6 Disk Lasers

A disk laser is a compact, highly efficient laser. It produces radiation of high power (1 kW or more). Applications lie in fields (cutting, welding, labeling), in competition with the Nd:YAG laser.

A disk laser (Fig. 15.7) consists of a disk (thickness 100–200 μm), pumped with a semiconductor laser. Because of the large diameter, the disk laser has a high beam quality. A large concentration of Yb^{3+} ions in Yb^{3+}:YAG allows for a compact design of the laser. We described the laser principle in the preceding section.

In comparison with a laser medium with a rod shape, the disk laser has a larger ratio of cooling area and active volume. The temperature distribution within the active medium has a nearly homogeneous radial distribution. This leads to a high beam quality.

A Nd:YVO_4 laser can be operated as miniature picosecond laser (Fig. 15.8). A semiconductor laser (808 nm) pumps the laser, which emits radiation at 1,064 nm. The laser can generate picosecond pulses (duration 10 ps) at a high repetition rate (e.g., 30 GHz). Mode locking is possible by use of a mirror with a reflectivity that depends on the radiation intensity. The reflectivity is small at small intensity and large at high intensity. The mirror is a semiconductor saturable absorber mirror (SESAM). A Nd:$GdVO_4$ laser has similar properties as the Nd:YVO_4 laser.

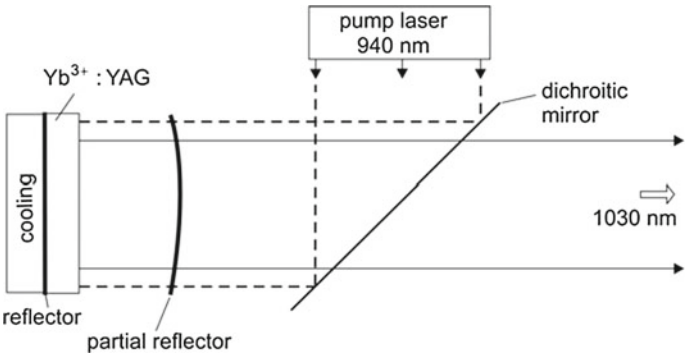

Fig. 15.7 Disk laser

Fig. 15.8 Picosecond disk laser

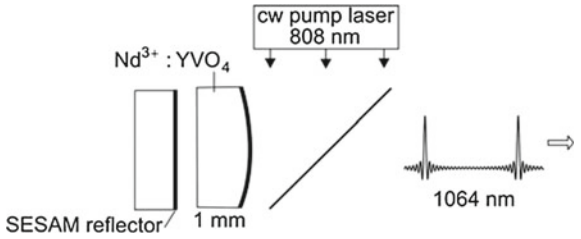

15.7 Fiber Lasers

Fiber lasers are important glass lasers. Fiber lasers have many applications in fields of material processing, chemistry, medicine, biology. The second harmonic radiation of glass fiber lasers serves for pumping of other lasers, e.g., of disk lasers. In comparison with other solid state lasers, fiber lasers are flexible and simple with respect to adjustment (or may not need adjustment at all).

The active medium of a fiber laser is a glass that is doped with rare earth ions. We describe here main features of a fiber laser (Fig. 15.9a):

- *Glass fiber* (length 1–10 m, or longer; diameter 5 μm), doped with ions.
- *Dichroitic end mirror*. It is highly reflecting for the laser radiation and transparent for the pump radiation.
- *Output coupling mirror*. In order to reach optimum efficiency, the reflectivity of the output coupling mirror is chosen appropriately.
- A fiber laser can be pumped with a semiconductor laser.

The pump waveguide either coincides with the laser waveguide (Fig. 15.9b) or has a larger diameter (Fig. 15.9c).

Fiber lasers are available in the 0.7–3 μm wavelength range. Rare earth ions in a glass occupy sites of different strength of the crystalline electric field. Therefore, the energy levels of the electronic states of ions in a glass are energetically distributed and the gain curves are broader than for rare earth ions in a crystal. The gain bandwidth can have a value of 10% of the center frequency of the gain curve.

Table 15.4 shows a list of fiber lasers:

- *Ytterbium-doped glass laser* (Yb^{3+} fiber laser). This laser generates radiation in a wavelength range near 1 μm.

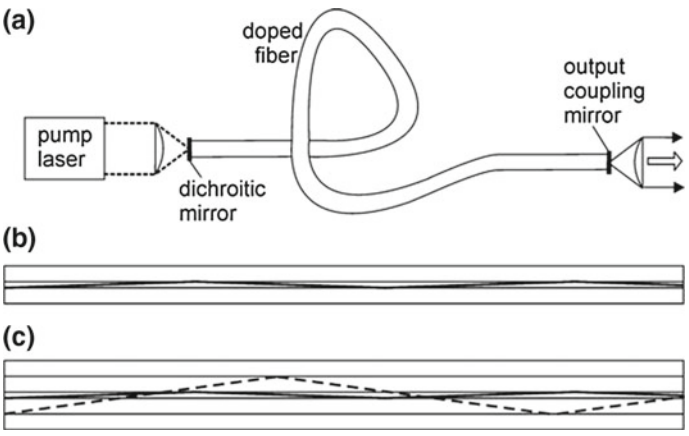

Fig. 15.9 Fiber laser. **a** Arrangement. **b** Fiber with coinciding pump and laser waveguide. **c** Fiber with pump and laser waveguide of different diameters

Table 15.4 Fiber lasers

Laser	λ (μm)	Doping % per weight
Yb^{3+} fiber	1.02–1.2	4
Yb^{3+}/Er^{3+} fiber	1.5–1.6	8/1
Yb^{3+}/Er^{3+} fiber	2.7–2.8	8/8
Tm^{3+} fiber	1.85–2.1	4
Ho^{3+} fiber	2.1 and 2.9	3

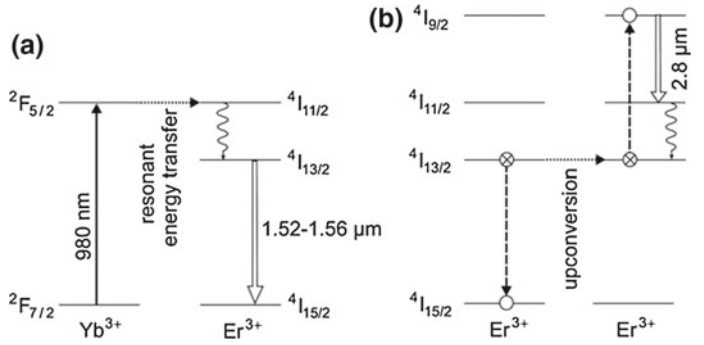

Fig. 15.10 Fiber lasers. **a** 1.5-μm erbium-doped fiber laser. **b** 2.8-μm erbium-doped fiber laser

- 1.5-μm *erbium-doped fiber laser* (Pr^{3+}/Er^{3+} fiber laser). The erbium-doped fiber laser makes use of the three energy levels $^4I_{15/2}$ (ground state), $^4I_{13/2}$ and $^4I_{11/2}$ of Er^{3+} (Fig. 15.10a). The 1.5-μm erbium-doped fiber laser is based on stimulated $^4I_{13/2} \rightarrow {}^4I_{15/2}$ transitions. The absorption coefficient for pump radiation is much larger if a glass contains, in addition to Er^{3+} ions, a large concentration of Yb^{3+} ions; the concentration can be ten times larger than the Er^{3+} concentration. The $^2F_4$ level of Pr^{3+} coincides with the energy level $^4I_{11/2}$ of Er^{3+}. Optical pumping and *resonant energy transfer* from Pr^{3+} ions to Er^{3+} ions leads to population inversion in the Er^{3+} ion ensemble. Co-doping with ytterbium enhances the absorptivity and allows for a more efficient optical pumping. The additional doping with ytterbium has only a small influence on the energy levels of the Er^{3+} ions.
- 2.8-μm *erbium-doped fiber laser* (Pr^{3+}/Er^{3+} fiber laser). The laser is pumped via Pr^{3+} ions. Above a concentration of about 1.5%, an excited Er^{3+} ion can transfer the excitation energy to a neighboring excited Er^{3+} ion by an *upconversion process*, leading to population of $^4I_{9/2}$ states (Fig. 15.10b). Laser radiation is due to $^4I_{9/2} \rightarrow {}^4I_{11/2}$ transitions.
- 2-μm *thulium-doped fiber laser* (Tm^{3+} fiber laser). Pumping results in population of $^3H_4$ levels (Fig. 15.11, left).*Cross relaxation* leads to population of $^3F_4$ levels; in a cross relaxation process, excitation energy is transferred to a neighboring unexcited ion (Fig. 15.11, center). Stimulated emission occurs by $^3F_4 \rightarrow {}^3H_6$

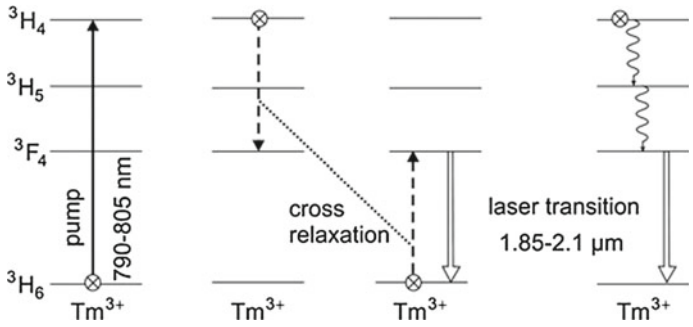

Fig. 15.11 2-μm thulium-doped fiber laser

transitions. Relaxation processes (Fig. 15.11, right) from $^3H_4$ to $^3F_4$ contribute additionally to population of the $^3F_4$ level.

- 2.1-μm and 2.9-μm Ho^{3+} doped fiber laser. Pumping is possible with radiation at 1.15 μm. The two laser transitions make use of the three lowest energy levels, namely the $^5I_8$ (ground state), the $^5I_7$, and $^5I_8$ states of Ho^{3+}.

We mention the energy transfer processes:

- Resonant energy transfer.
- Upconversion.
- Cross relaxation.
- Phonon-assisted energy transfer (Chap. 18).

Transfer of the excitation energy from an ion to another ion determines the microscopic dynamics of fiber laser media. We will treat the basis of energy transfer and the role of energy transfer processes in the microscopic dynamics of fiber media in Chap. 18. The treatment of the dynamics will provide the gain coefficient.

It is possible to use optically pumped fibers as amplifiers of radiation (Sect. 16.9 and Chap. 18). A special amplifier is the erbium-doped fiber amplifier—used in the optical communications. It is also possible to pump the active medium of an erbium-doped fiber amplifier with radiation at a wavelength (1.48 μm) that is only slightly smaller than the wavelengths (1.52–1.56 μm) of the range of gain (Chaps. 18 and 33.4).

15.8 A Short Survey of Solid State Lasers and Impurity Ions in Solids

The basic solid (a crystal or a glass) of a solid state laser (Fig. 15.12) is transparent for pump and laser radiation. The solid acts as a host of impurity ions. The electric field (crystal field) at the site of an impurity ion in a crystal or in glass mainly determines the energy levels of an impurity ion.

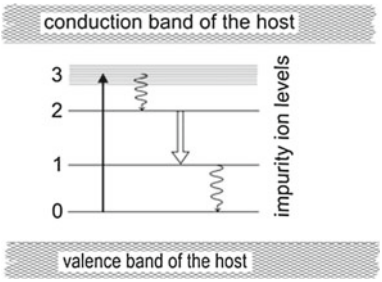

Fig. 15.12 Solid state laser: energy levels

Table 15.5 Maximum doping concentrations

Laser	λ (μm)	wt.%	N_0 (m^{-3})
Nd:YAG	1.06	1	1.4×10^{26}
Nd:YVO_4	1.06	1	1.5×10^{26}
Nd:YLF	1.05	1	1.3×10^{26}
Nd:glass	1.05	3.8	3.2×10^{26}
Yb:YAG	1.06	6.5	9×10^{26}
Pr:YAG	1.03	26	2.7×10^{28}
Er:YAG	2.8	0.7	1×10^{26}
Er:glass	1.5	3	2×10^{26}
Cr:Al_2O_3	0.69	0.05	1.6×10^{25}
Cr:LiSAF	0.9	15	1.5×10^{27}
Cr:LiCAF	0.8	15	1.5×10^{27}
Ti:Al_2O_3	0.83	0.1	3.3×10^{25}

Table 15.5 shows a list of few host crystals and impurity ions. The maximum concentration of impurity ions in a solid depends on the properties of the both solid and the impurity ions. Maximum doping concentrations lie between 0.1% by weight (Ti^{3+} in Al_2O_3) and 26% by weight (Pr^{3+} in YAG):

- Sapphire (Al_2O_3). The crystal field splitting of the 3d state of Ti^{3+} and the interaction of the electronic states with the lattice vibrations (phonons) are the basis of the titanium–sapphire laser.
- YAG (yttrium aluminum garnet = $Y_3Al_5O_{12}$). This material grows in a very high crystal quality. Doping with all three-valid rare earth ions is possible. Doping ions replace Y^{3+} ions. The doping concentration has a value of about 1% for all but two rare earths: the doping with Pr^{3+} can be exceptionally high (25%) and also the doping with Yb^{3+} can be very high (6%).
- YVO_4 (yttrium vanadium oxide). This host material became available in the last years as a high-quality crystalline material.
- $CaWO_4$, CaF_2, LaF_3 doped with rare earths can also be used as laser media.
- $LiYF_4$, LiSAF, LiCaF (Sect. 15.5).
- Alkali halides in color center lasers.

Doping of a solid with impurity ions creates the basic electronic states used in active media. Another possibility is the use of color centers. The following list gives a short survey of defect centers (ions and color centers) contained in various laser media:

- *Ions with valence electrons*. The ions of the transition metals (Ti^{3+}, Cr^{3+}, V^{3+}) have 3d electrons, which are strongly influenced by the crystalline electric field. The energy levels are vibronic levels.
- *Rare earth ions*. Three-valid ions (Nd^{3+}, Er^{3+}, Ho^{3+}, Pr^{3+}) as well as two-valid ions are suitable as impurity ions of laser media. The ions of the rare earths have closed external shells ($5s^2 5p^6$) and (internal) 4f states. A crystal field leads to a splitting of the 4f levels. The gain bandwidth of rare earth doped crystals at room temperature is of the order of 100 GHz (Sect. 15.9). The rare earth ions are excited via 4f levels or other energy levels. The crystal field splitting depends on the symmetry of the site of an impurity ion in a host material and on the lattice parameters of the host. Therefore, the wavelength of laser radiation, which is due to transitions between two particular energy levels of impurity ions, depends on the host material.
- *Color centers.* There are many different color centers. A color center can be an F center, which is an electron on an empty halide ion site in an alkali halide crystal, replacing the negative ion in an ionic crystal (LiF, NaF, KF, NaCl, KCl, CsCl). However, F centers that can be produced by irradiating a crystal with X-rays are not suitable as defect centers of active media. Suitable as laser media are alkali halides that contain F_2^+ centers. An F_2^+ center consists of two adjacent empty halide ion sites occupied with one electron. An F_2^+ center may be compared with an H_2^+ molecule. The electronic energy levels of an F_2^+ center are strongly influenced by the crystal surrounding: the electronic states of an F_2^+ center are vibronic states; for a discussion of vibronic lasers, *see* Chap. 17. The color center lasers are tunable. Different host crystals lead to different emission bands in the near infrared (from 0.8 to 4 μm). Most of the color center lasers require cooling to liquid nitrogen temperature. Today, color center lasers cannot compete with semiconductor lasers.

The laser medium can have, as we already mentioned, various geometrical shapes:

- *Circular cylindric rod*. There is a temperature gradient perpendicular to the rod axis; the rod is cooled mainly via the cylindric surface. The gain factor can be large.
- *Disk*. There is a temperature gradient perpendicular to the disk axis; the disk is cooled mainly via one of the plane surfaces.
- *Fiber*; Sect. 15.7 and Chap. 18.

Table 15.6 shows a selection of doping ions. The energy levels of the transition metals have electrons in 3d states. These are strongly influenced by the crystalline electric field giving rise to strong splitting of the energy levels and to strong vibronic sidebands (Chap. 17). A crystalline electric field splits the energy levels of a rare earth ion, too. However, the splitting energy is much smaller and vibronic sidebands are weak.

Table 15.6 A selection of ions

Atomic number	Element	Ion	Configuration
22	Titanium	Ti^{3+}	$3d\ ^2D_{3/2}$
24	Chromium	Cr^{3+}	$3d^3\ ^4F_{3/2}$
59	Praseodymium	Pr^{3+}	$4f^2\ ^3H_4$
60	Neodymium	Nd^{3+}	$4f^3\ ^4I_{9/2}$
64	Gadolinium	Gd^{3+}	$4f^3\ ^8S_{7/2}$
68	Erbium	Er^{3+}	$4f^{11}\ ^4I_{15/2}$
69	Thulium	Tm^{3+}	$4f^{12}\ ^3H_6$
70	Ytterbium	Yb^{3+}	$4f^{13}\ ^2F_{7/2}$

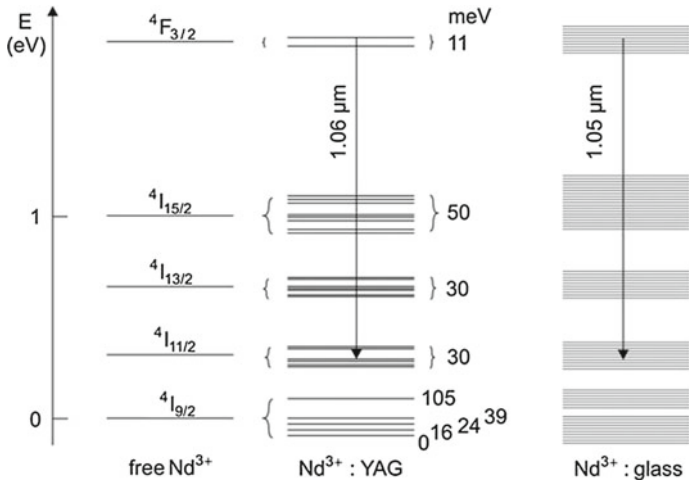

Fig. 15.13 Energy levels of Nd^{3+}

As an example of crystal field splitting of energy levels of a rare earth ion, we show energy levels of Nd^{3+} (Fig. 15.13):

- Free Nd^{3+} ion. The $4f^3$ state splits into states with different total angular momentum (quantum number J), due to spin–orbit interaction. The ground state is $^4I_{9/2}$. Optical transitions are forbidden.
- Nd^{3+}:YAG. The crystalline electric field splits a level with the quantum number J into $(2J + 1)/2$ sublevels (*Stark splitting*); a rare earth ion with an odd number of 4f electrons shows a twofold degeneracy (*Kramers degeneracy*)—*see*, for instance, [121]. The splitting of the sublevels has values in the range of several meV to about 100 meV [122–126]. Optical transitions are allowed due to spin–orbit interaction or due to the interplay of spin–orbit interaction and crystalline electric field. The strongest transition is a transition between a $^4F_{3/2}$ sublevel and a $^4I_{11/2}$ sublevel. The corresponding line (at 1.064 µm) has a linewidth of 12 GHz

Table 15.7 Gain data of Nd^{3+}:YAG and Nd^{3+}:glass

Laser	λ (μm)	$\Delta\nu_g$	τ_{sp} (μs)	σ_{21} (m^2)
Nd^{3+}:YAG	1.064	140 GHz	230	3×10^{-22}
Nd^{3+}:glass	1.054	7 THz	300	7×10^{-24}

at room temperature. The values of the crystal field splitting of levels of Nd^{3+} in other crystals are of the same order.

- Nd^{3+}:glass. Because of the great variety of the crystal field acting on ions at different sites in a glass, the energy of a sublevel differs strongly for ions at different sites—we obtain a continuous energy distribution of sublevels. The strongest transition is again a transition between a $^4F_{3/2}$ sublevel and a $^4I_{11/2}$ sublevel. The corresponding line (with the center near 1.054 μm) has a linewidth (7–10 THz) that is large and depends on the composition of the glass.

Table 15.7 shows data of Nd^{3+}:YAG and Nd^{3+}:glass. The gain cross section of an Nd^{3+} ion in a glass is 40 times smaller than the gain cross section of an Nd^{3+} ion in a YAG crystal.

15.9 Broadening of Transitions in Impurity Ions in Solids

Various broadening mechanisms can be responsible for the shape of the gain profile of an active medium based on optical transitions between two levels of an impurity ion in a solid:

- *Line broadening due to phonon Raman scattering*. An electronic transition is accompanied by a phonon Raman scattering process, i.e., by inelastic scattering of a phonon during the emission of a photon (Fig. 15.14). This process is frozen out at low crystal temperature (e.g., at 4 K or 77 K) but is the main broadening mechanism of many transitions in impurities in crystals at room temperature. Phonon Raman scattering leads to homogeneous line broadening. Fluorescence as well as absorption line have Lorentzian shape. We can interpret the mechanism as line broadening due to elastic collisions of an atom with phonons.

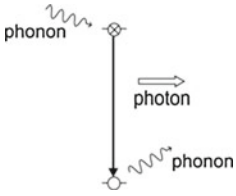

Fig. 15.14 Optical transition accompanied with phonon Raman scattering

Examples 1.06-μm line of Nd^{3+}:YAG at room temperature; the R_1 and R_2 lines of ruby at room temperature.

- *Line broadening due to the Stark effect*. Due to the Stark effect, the energy levels of ions at different sites of impurity ions in a glass have an energy distribution—and the transition energies too. Phonon-assisted energy transfer processes create a quasiband of excited ions (Chap 18).

At low temperature, the Stark effect of impurity ions in a solid (crystal or glass) leads to inhomogeneous broadening of absorption lines. An impurity ion occupies not exactly the position of an ion that it replaces. The strength of the crystal field at different impurity ion sites is slightly different. Due to the Stark effect, the energy levels and transition energies of the ions at different sites are different. The lineshape can be Gaussian.

Examples almost all lines that are due to transitions between 4f states of ions in crystals at low temperature (e.g., at 4 K); the R lines of ruby at low temperature; all lines of impurity ions in glasses at low temperature.

References [1–4, 6, 11, 31, 120–126].

Problems

15.1 Ruby laser.

(a) The crystal of a Q-switched ruby laser is optically pumped by the use of a flash lamp so that almost all Cr^{3+} ions are excited. Estimate the energy and the power of a laser pulse of 100 ns duration. [*Hint*: ignore oscillations that could cause a temporal structure in the pulse shape].

(b) Laser oscillation is possible with a ruby crystal cooled to low temperature (4 K) with two plane parallel surfaces as reflectors (refractive index of ruby $n = 1.76$). Estimate the threshold pump power of a laser with a ruby crystal (length 1 cm) pumped in a volume of 0.2 mm diameter by another laser (pump wavelength 530 nm); at low crystal temperature, the R_1 and R_2 lines are 100 times narrower than at room temperature.

15.2 Gain cross sections. Determine, by use of the data of linewidths and spontaneous lifetimes, the ratio of the gain cross section of the 1.06 μm line of Nd^{3+}:YAG and of the gain cross section at the line center of Ti^{3+}:Al_2O_3.

15.3 Titanium–sapphire laser. Why is the energy distribution of vibronic energy levels of Ti^{3+} in Al_2O_3 continuous while the vibronic energy levels of N_2 are discrete?

15.4 Laser tandem pumping. A femtosecond titanium–sapphire laser can be pumped with the frequency-doubled radiation of a Nd^{3+}:YVO_4 laser, which itself is pumped by use of a semiconductor laser.

(a) Estimate the quantum efficiency of such an arrangement if the frequency doubling has a power conversion of 50%.
(b) What is the advantage of the tandem pumping in comparison with the direct pumping of the titanium–sapphire laser with a semiconductor laser?

15.5 Fiber laser. Estimate the efficiency of an erbium-doped fiber laser pumped with a pump power twice the threshold pump power.

15.6 Explain the nomenclature ($^4I_{9/2}$, $^4I_{11/2}$, $^7F_{7/2}$ etc.) used for characterization of atomic states.